Geomechanics and Engineering, *Vol. 18, No. 2 (2019) 189-203*
DOI: https://doi.org/10.12989/gae.2019.18.2.189

Thaw consolidation behavior of frozen soft clay with calcium chloride

Songhe Wang*[1], Qinze Wang[1b], Jian Xu[2a], Jiulong Ding[1b], Jilin Qi[3a], Yugui Yang[4a] and Fengyin Liu[1a]

[1]Institute of Geotechnical Engineering, Xi'an University of Technology, Xi'an, Shaanxi, 710048, China
[2]School of Civil Engineering, Xi'an University of Architecture and Technology, Xi'an, Shaanxi, 710055, China
[3]College of Civil and Transportation Engineering, Beijing University of Civil Engineering and Architecture, Beijing 100044, China
[4]State Key Laboratory for Geomechanics and Deep Underground Engineering, China University of Mining and Technology, Xuzhou, Jiangsu 221008, China

(Received January 9, 2019, Revised May 16, 2019, Accepted May 28, 2019)

Abstract. Brine leakage is a common phenomenon during construction facilitated by artificial freezing technique, threatening the stability of frozen wall due to the continual thawing of already frozen domain. This paper takes the frequently encountered soft clay in Wujiang District as the study object, and remolded specimens were prepared by mixing calcium chloride solutions at five levels of concentration. Both the deformation and pore water pressure of frozen specimens during thawing were investigated by two-stage loading tests. Three sections were noted from the changes in the strain rate of specimens during thawing at the first-stage load, i.e., instantaneous, attenuated, and quasi-stable sections. During the second-stage loading, the deformation of post-thawed soils is closely correlated with the dissipation of pore water pressure. Two characteristic indexes were obtained including thaw-settlement coefficient and critical water content. The critical water content increases positively with salt content. The higher water content of soil leads to a larger thaw-settlement coefficient, especially at higher salt contents, based on which an empirical equation was proposed and verified. The normalized pore water pressure during thawing was found to dissipate slower at higher salt contents, with a longer duration to stabilize. Three physical indexes were experimentally determined such as freezing point, heat conductivity and water permeability. The freezing point decreases at higher salt contents, especially as more water is involved, like the changes in heat conductivity. The water permeability maintains within the same order at the considered range of salt contents, like the development of the coefficient of consolidation. The variation of the pore volume distribution also accounts for this.

Keywords: thaw consolidation; frozen soil; freezing point; heat conductivity; water permeability

1. Introduction

Massive infrastructures have been constructed with growing needs in underground space utilization and exploitation of natural resources since the last century (Ma *et al.* 2011, Marwan *et al.* 2016, Tengborg and Sturk 2016, Nelson 2016, Xu *et al.* 2018), e.g., the subways in the Yangtze River Delta region, China. However, the subway construction in this region has to tackle with one of the problematic soils, i.e., soft clay, due to its poor engineering properties (Karstunen *et al.* 2006, Yazdani and Mohsen 2012, Park 2016). This kind of soil is not that suitable to be used as the foundation, and requires foundation treatment by means of two frequently used methods such as preloading drainage consolidation or chemical grouting (Quang and Giao 2014, Yildiz and Uysal 2015). The former in general takes a long duration for soils to be consolidated to a satisfied degree while the latter has an inevitably negative effect that chemical substances intruded the ground and were hardly eliminated, although a reliable protection for underground excavation can be guaranteed (Chen 1996). In this case, the artificial freezing technique has been increasingly utilized as an important substitute (Wang *et al.* 2005, Vitel *et al.* 2016). However, the accidents happened in Guangzhou and Shanghai Metro have rang the alarm for us that the brine leakage occurred at the fractured part of the freezing pipe should be paid more attentions. The contingency plan should be specially constituted. Although the brine leakage cannot instantly jeopardize the engineering safety, the extension of frozen wall as well as the strength of frozen soils will be affected after brine intrusion. More notably, the structural integrity of frozen wall can be hardly preserved due to the continual thawing of frozen soils, and larger ground subsidence therefore can be induced. Thus, the investigation of thaw consolidation behavior of frozen saline soils should be carried out to prevent this kind of potential safety hazard.

Two-stage thaw settlement test suggested by Tsytovich (1975) was mostly employed in early studies by using the confined compression apparatus with 1D temperature control. One of the characteristic indexes, i.e., thaw settlement coefficient can be conveniently determined. Besides, the freeze-thaw test apparatus produced in recent decades has been successfully applied in experimental researches in frozen soil mechanics, with the merits of both specimen size increase and inclusion of complex thermal boundaries. The newly developed transducers for

*Corresponding author, Ph.D.
E-mail: wangsonghe@126.com
[a]Ph.D.
[b]Ph.D Student

http://www.techno-press.org/?journal=gae&subpage=7
ISSN: 2005-307X (Print), 2092-6219 (Online)

temperature, water and displacement to a large extent improves the live monitoring efficiency of heat and water migration as well as the displacement during thaw consolidation. Happily we have found the high-precision transducers with better load bearing and water-proof capacity have been used in recent works. In engineering activities, the coefficient of thaw settlement was used in representing the magnitude of thaw settlement of frozen soils, and can be simply calculated by an empirical equation, i.e., $A_0=\Delta h/h_0$, with Δh as the settlement of thawing domain under gravity and h_0 as the thawing depth. Experiments prove that the thaw settlement coefficient depends on multiple factors such as dry density, water content, particle grading characteristics, and the Atterberg limits (Hildebrand 1983, Nelson *et al.* 1983, Ponomarev *et al.* 1988, Panday and Corapcioglu 1995). Empirical equations for the above were proposed to estimate the coefficient of thaw settlement. Early works focused on its dependence on dry density, porosity and water content, with statistical equations fitted. In the meanwhile, the equations solely based on one factor such as water content or dry density were developed. However, the complex correlations that have been proven in previous experiments necessitate a more reasonable mathematical description (Wang *et al.* 2016a).

Consolidation of post-thawed domain under gravity and overburden pressure with water discharged should also be taken into account. Estimation of deformation of thawing soils will be underestimated if the second part is neglected. Morgenstern and Nixon (1971) firstly derived a 1D consolidation theory for thawing soils with a predefined moving thawing boundary. Then this assumption is improved by incorporating a more complex thawing boundary by Nixon and Morgenstern (1973). Foriero and Ladanyi (1995) further revised the theory with a large-strain consolidation theory included and the first stage of thaw consolidation that can be classified as the large-strain problem can be well modeled. Sykes *et al.* (1974) extended the 1D theory into 3D conditions and the release of latent heat during ice-water phase change can be conveniently modeled by a simple term like heat source so that the complex heat and water migration as well as the stress state can be well simulated. Shoop (2005) modeled the deformation of thawing soils under conventional traffic loads by using an elastic-plastic cap model in ABAQUS platform. Yao *et al.* (2012) derived a 3D large-strain consolidation theory for thawing permafrost considering the volume and shape change and used to predict the thawing settlement of embankment in Qinghai-Tibet highway. Wang and Liu (2015) modeled the thaw consolidation behavior of frozen soils at various thermal boundaries by using an improved von Wolffersdorff hypoplastic model (von Wolffersdorff 1996) with a tensorial term representing the cohesion of frozen sand and a modified Richards equation. Wang *et al.* (2016b) gave a reasonable description of thaw consolidation in 1D condition with a periodical thermal boundary considered. Yao *et al.* (2016) investigated the distribution and dissipation of pore water pressure during thawing of frozen soils. From previous work, the effect of soluble salt has not been considered in testing, e.g., the effect of soluble salt on thaw settlement coefficient and pore water pressure dissipation. Experiments have proven that the viscosity of pore fluid and freezing point of soils will be affected by the solutes in pore solution (Wang *et al.* 2018). This may further influence the thaw consolidation behavior. More importantly, investigation of thaw consolidation of frozen saline soils will facilitate the artificial ground freezing, especially when soluble salt is included, e.g., the estimation of thaw settlement of ground after brine leakage induced by fractured freezing pipes.

Considering the negative effect of salt inclusion on the stability of frozen wall, this paper takes the frequently encountered soft clay in Wujiang District as study object to prepare saline specimens by adding calcium chloride solution. Thaw consolidation tests were carried out in an apparatus by which the ambient temperatures can be accurately controlled. Thaw consolidation behavior was investigated including the coefficient of thaw settlement and pore water pressure, as well as their correlations with water and salt. Three of the correlated indexes such as freezing point, heat conductivity and water permeability were discussed in view of the influence of soluble salt. The changes in soil pore structure during thawing were analyzed based on the mercury intrusion (MIP) test.

2. Test program

2.1 Soil specimen preparation

Soil samples were taken from a foundation pit close to the Wujiang Metro at a depth of 5.0 to 6.0 m. According to the standard of soil test method (GB/T50123-1999), the physical indexes of the taken samples can be measured in laboratory. The initial ion contents were determined by ion chromatography and titration. The basic physical and chemical indexes are listed in Table 1. It indicates a low initial content of soluble salts in this soft clay and its negative influence on specimen preparation and subsequent thawing behavior can be neglected.

The samples air-dried were firstly crushed and sieved through a 2-mm sieve, and was then put into a dryer. The calcium chloride solutions were prepared by mixing the anhydrous calcium chloride with purity of 95% and deionized water, and were subsequently placed into a closed and water-proof environment for 24 h. Then the dried soils and calcium chloride solutions was mixed and kept in a constant temperature and humidity room for 24 h to ensure the uniformity of water and salt. According to the targeted dry density, water and salt contents, the specimens used in testing are all remolded by five-layer static compression of the prepared slurry in a high-strength plexiglass tube. The diameter and height of the specimens are both controlled to be 10.0 cm.

The salt content of soil specimens was controlled to be 0.0%, 0.2%, 0.5%, 1.0%, 2.0% and 5.0%, respectively. Six levels of water content were considered here, i.e., 10.0%, 20.0%, 30.0%, 40.0%, 50.0% and 60.0%. The dry density was controlled to be 1.70 g/cm^3 to eliminate the discrepancy caused by the variability of dry densities among soil specimens. In order to verify the rationality of the specimen preparation procedure, three to five specimens were randomly selected to measure the water content by over

Table 1 Physical indexes and ion contents for soft clay samples

Physical parameter	value	Ions	value / %
Natural water content, w_n/%	49.3	Anions	
Dry density, ρ / g/cm^3	1.70	CO_3^{2-}	0
Specific Gravity, G_s	2.70	HCO_3^-	0.0023
Atterberg limit		Cl^-	0.0032
Liquid limit, w_L /%	41.8	SO_4^{2-}	0.0067
Plastic limit, w_p/%	21.6	total	0.0122
Compaction test		Cations	
Optimum water content, w_{opt} / %	18.9	K^+	0.0011
Maximum dry density, ρ_{dmax} / g/cm^3	1.75	Ca^{2+}	0.0017
Particle grading characteristics		Na^+	0.0052
0.075-2.0 mm	7.5%	Mg^{2+}	0.0009
0.005-0.075 mm	71.5%	total	0.0089
<0.005 mm	21.0%		

drying method and after weighing the dried specimens, the dry density can be calculated. The difference of dry density among soil specimens was controlled to be less than ±0.01 g/cm^3 while less than ±1.0% for the water content. Then the salt content of the dried specimen was obtained by salt leaching and proves a maximum difference of 0.04%.

(1) Thaw consolidation test

The apparatus used in thaw consolidation testing has an effective volume of 400.0 L. The temperature is applied by means of compressor cooling, with a range of -60 - 100 ºC and a precision of ±0.3 °C. The physical appearance and schematic diagram of the apparatus are illustrated in Fig. 1. The 3D temperature control can be fulfilled by improving the apparatus. The transducers for temperature, displacement and water can be directly connected with the preset position of the specimen to live monitor the thawing behavior of soil specimens, with the data live recorded by a data logger. The availability of water can be accessed by a Mariotte bottle that has been connected to the test chamber. Here, the tests were carried out with not water supply. Before testing, the specimen prepared together with the plexiglass tube was frozen in a cryostat and the ambient temperature is adjusted to be -20 ºC. The duration is not less than 6 h to ensure a minimum volumetric deformation during a fast freezing process. The frozen specimen was quickly mounted on the pre-cooled test chamber of freeze-thaw test apparatus. Transducers for temperature and pore water pressure were inserted into the preset positions of the specimen through the plexiglass tube. Afterwards, the upper plate made of oxidation-resisting steel was placed on the top of specimen with the displacement transducer set. The temperature of the upper plate was adjusted as -10ºC and then increased to +10ºC as the temperature stabilized. In the meanwhile, thaw consolidation of the frozen specimen initiated with an overburden pressure of 1.0 kPa applied on the upper plate. The deformation, pore water pressure and temperature were live monitored until a stable deformation was reached. The second-level load was exerted on soil specimen just as the first stage was completed, with the magnitude of 50.0 kPa. Test data was successively monitored and recorded, with the duration longer than 12 hours. Note that it is appropriate to select a lower freezing temperature for frozen wall before designing the freezing system so that the bearing capacity of frozen wall can be guaranteed and benefit for the excavation of core soils. For soils in the Yangtze River Delta region, the temperature for freezing can be taken as -10ºC when the excavation depth is not larger than 30 m, and thus the cold end is adjusted as -10ºC during testing.

A 3D fast freezing mode was utilized during freezing to avoid the excess migration of both water and salt in each direction and to further minimize the negative influence of the inconsistency among soil specimens on thawing behavior. Specimens at four typical water-salt combinations, i.e., T1 (w=30.0%, η=0.2%), T2 (w=30.0%, η=5.0%), T3 (w=60.0%, η=0.2%) and T4 (w=60.0%, η=5.0%), were selected to verify the rationality of this freezing mode in confining both the water and salt during freezing stage. Firstly, the specimen was cut into five uniform layers with the thickness of each layer equal to 2.0 cm. Each layer was divided into four quadrants, and the schematic diagram is shown in Fig. 2(a). The water content of each part was tested by oven drying, and the salt content of the dried portion was obtained by salt leaching, with the contours of both water and salt after freezing illustrated in Figs. 2(b)-2(e). From the figure, the water in soil tends to be accumulated from the middle to the both ends of soil specimen in this freezing mode and the maximum deviation of each layer along the height of the specimen does not exceed 3%. Besides, within the same layer, the water content of the specimen varies within a narrow range and the maximum difference is about 1%. Figs. 2(d) and 2(e) show that for soil specimens at salt contents of 0.2% and 5.0%, phenomena like the changes in soil water can be observed, i.e., higher salt contents appear in both ends of the soil. While a decreasing trend noted at the central part in general. However, the variation of the salt content with the height of the specimen is more complex at a lower level even if only a deviation of 0.1% noted. While for those at higher contents, an obvious zonal distribution can be noticed at each layer, with the maximum deviation higher than those at lower contents. A more uniform distribution of salt also exists at each layer with the maximum difference lower than 0.3%. Soluble salt in general exhibits simultaneous migrations with soil water and in most cases migrates towards the outside of soil specimen during 3D fast freezing. Since the specimen is divided into four uniform right-angled sectors at the same layer, the water and salt migration within each layer cannot be reflected. It proves that by using this mode to freeze, the water in soil can be quickly frozen and locked in the pores, and the water that migrates will be very limited, that is, the part of the unfrozen water that can carry the salt migration, so the salt migration can be limited to a very small range. This can provide a relatively uniform water and salt profile that is also a good basis for explaining the deformation of frozen saline soft clay during thawing.

(2) Thermophysical and hydraulic tests

Previous work indicates that the engineering properties of soils will be changed considerably as the soluble salt

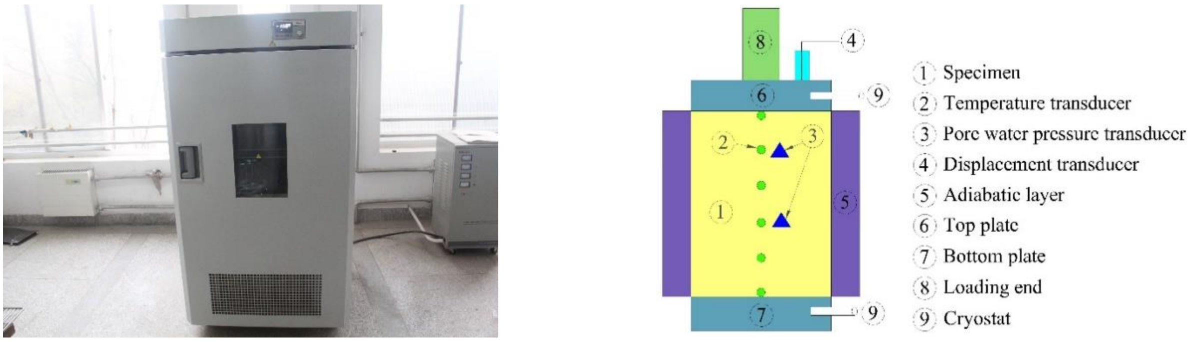

(a) Physical appearance (b) Schematic diagram

Fig. 1 Apparatus for thaw consolidation testing

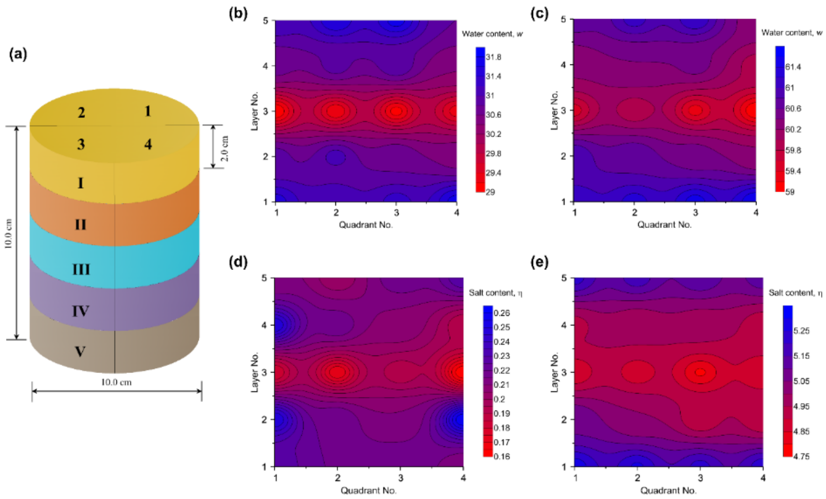

Fig. 2 Schematic diagram of soil specimen division and contour of water and salt distribution in a 3D fast freezing mode: (a) division of soil specimen, (b) w=30.0%, (c) w=60.0%, (d) η=0.2% and (e) η=5.0%

intruded (Kozlowski 2009, Bing and Ma 2011). Thaw consolidation behavior of frozen saline soils will be affected that can be inferred from the experiments above. To reveal the effect of salt content on heat migration during thawing, both the freezing point and heat conductivity were measured in laboratory. For the former, the freezing point that determines whether soils are frozen or not was obtained by the classic cooling curve method proposed by Grechishchev *et al.* (2001). The temperature of coolant is pre-cooled to -20 ºC before the soil specimen was placed into, aiming to produce a uniform negative temperature environment. Then the specimen was placed into the cryostat with the duration not less than 4 h. The temperature in the soil was monitored by a high-precision transducer and collected by a data logger. The precision for the transducer is ±0.01ºC.

The heat conductivity for specimens was measured by the transient hot-wire technique. The test apparatus includes the hot-wire sensors, measuring instrument and matched computer. The measuring instrument is equipped high-precision thermal probes. Before testing, small holes were drilled in the specimen and a closed environment was produced with preservative film wrapped up. Specimens were quickly transferred to the measuring instrument with thermal probes inserted. Meanwhile, the given electric current was imposed on with the relationship of temperature and time recorded. The coefficient of heat conductivity for specimens can be calculated by graphs plotting temperatures with time logarithm. Specimens cut from the taken soil samples are sized at 200 mm×100 mm×50 mm. Both the water content and dry density are identical to those in tests above. The target temperatures are -20, -10, -5, 0, 5, 10 and 20 ºC.

Specimens used in permeability testing were cut from the post-thawed soils, with diameter of 61.8 mm and height of 40.0 mm. A varying-head infiltration test was carried out to obtain the permeability of post-thawed saline soft clay. Firstly, the cutting ring was placed into a closed chamber and specimens were saturated in a vacuum system for 20 h. Note that the calcium chloride solution with the salt content identical to the specimen is used in both vacuum saturation and infiltration tests.

(3) Mercury Intrusion Porosimetry (MIP) tests

The pore volume distribution curves of saline soft clay during a freeze-thaw cycle are obtained by the AutoPore IV 9500 Automatic mercury intrusion porosimetry with the resolution range of 360-0.005 μm. Thus, the changes in the seepage channel in the soil can be analyzed. The pore structure of the specimen can be obtained by pressing mercury into the tested specimen under a growing external pressure during the mercury intrusion testing. According to the Washburn equation (Webb 2001), the relationship

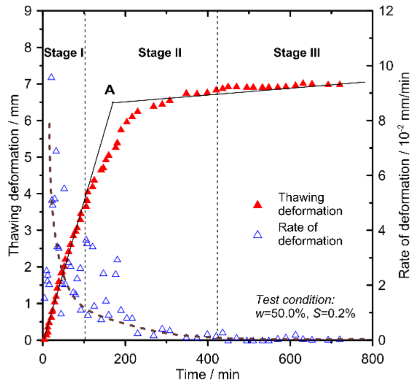

(a) Deformation and deformation rate

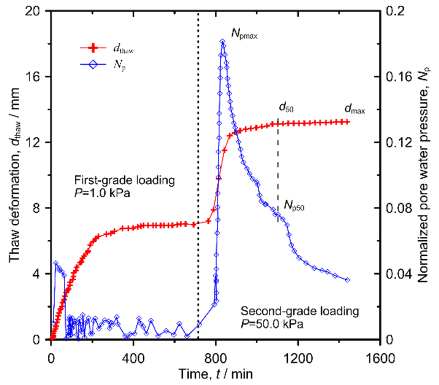

(b) Deformation and pore water pressure

Fig. 3 Stages of thaw settlement of frozen saline soft clay

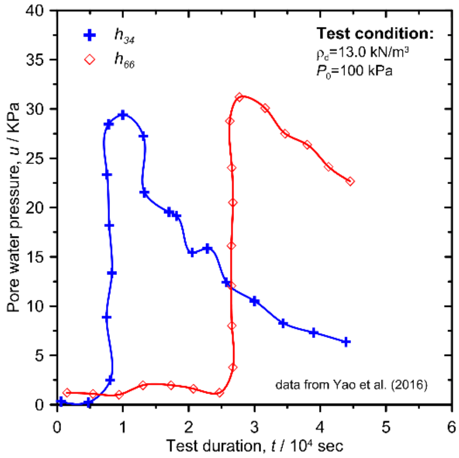

Fig. 4 Pore water pressure dissipation of silty clay during thawing (Yao *et al.* 2016)

between the applied pressure and the cylindrical pore radius can be obtained by Eq. (1).

$$p = -2\sigma \cos\alpha / r \tag{1}$$

where, p is the applied mercury intrusion pressure (psia), with the unit of psia equal to 6.8948 kPa; σ is the coefficient of surface tension (N/m), which can be taken as 0.484 N/m; α is the mercury intrusion angle (°), equal to 130°; r is the radius of cylindrical pores (m).

First, soil specimens before freezing and after thawing were cut into several clods sized at 1.0 cm × 1.0 cm × 1.0 cm by a wire saw, and rapidly frozen in liquid nitrogen to directly convert the pore water into a crystal. Vacuuming makes it directly sublimate from the crystal, thereby ensuring that the pores in the soil do not shrink due to dehydration. The mercury intrusion test was carried out after the specimen was dehydrated. Here, the soil specimens at salt contents of 0%, 0.5% and 5.0% were tested.

3. Test results

3.1 Stages of thaw consolidation for frozen saline soft clay

In practical engineering, multiple types of ice exist in frozen ground, e.g., cemented ice and segregated ice. As the ground is warming, the underlain frozen soils tend to thaw, with larger pores produced and easily compressed under gravity and overburden pressures, accompanied by the dissipation of post-thawed soil water. Especially in ice-rich ground, thawing of frozen ground may induce considerable thaw settlement, and the service life of infrastructures that were constructed above may be reduced. Here, we firstly analyzed the stages of thaw settlement of frozen saline soft clay at the first-stage load, as illustrated in Fig. 3(a). It is easily noticed from the figure that the deformation of frozen saline specimens during thawing exhibits the nonlinear increase, and can be classified into three stages based on the variation of strain rate. The first is the instantaneous deformation stage, with a rapid compression of soil structure under load due to the thawing of ice in various types. During this stage, the deformation rate is maintained at an approximately high level and this can be regarded as the thaw settlement of frozen soils. The second is the attenuated deformation stage, with a declined rate of deformation, reflecting the reorganization and reorientation of soil particles. Note that the pore water is discharged from soil pores until a relatively stable rate of deformation is reached, i.e., the third stage with a continual consolidation of thawing soils at the first stage, within which the rate tends to minimize, resulting in a more stable soil structure.

Both the deformation and pore water pressure during thawing at the two-stage loading conditions were plotted in a graph to further analyze the development of pore water pressure and its correlation with deformation, as shown in Fig. 3(b). The concept of normalized pore water pressure, N_p proposed by Yao *et al.* (2016) is introduced in Eq. (2).

$$N_p = \frac{u}{p_0} \tag{2}$$

where, u is the pore water pressure of specimen during thawing (kPa); p_0 is the overburden pressure (kPa). It shows that at the first stage of loading, the pore water pressure varies within a narrow range of not higher than 1.0 kPa, especially as the consolidation of thawing specimen stabilized. At a relatively low overburden pressure, little influence of pore water pressure can be observed while the deformation of soil specimen in this stage mainly results from the settlement of thawing soils due to ice-water phase change. The pore water pressure instantly grows as the second-stage load was applied on specimen and the normalized pore water pressure N_p reached the peak value of 0.18 within a short duration. Correspondingly, considerable deformation of specimen rapidly occurred. This is closely related to the secondary compression of soil skeleton that has also induced a substantial increase in the pore water pressure. Then the pore water pressure of post-thawed domain was dissipated with the consolidation of soils. This can also be found from the experiment that carried out on silty clay taken from the Qinghai-Tibet plateau (Yao *et al.* 2016), as presented in Fig. 4. For the frequently encountered silty clay in the Qinghai-Tibet plateau, the live monitoring data of pore water pressure at two conventional loads of 50 and 100 kPa, indicates that as the thawing boundary intruded the frozen domain, a rapid growth of pore water pressure will be noted under the dual effect of gravity and overburden pressure. Then it stabilized accompanied with a relatively stable deformation. Besides, the peak value of pore water pressure depends on the load level, i.e., higher pore water pressure occurred at high stress conditions. In the meanwhile, the pore water pressure dissipated at a relatively low rate, similar to the experiments carried out in this study.

3.2 Thaw-settlement coefficient

Tsytovich (1985) proposed a two-stage thaw settlement test method to facilitate researches in thaw consolidation of frozen soils. The testing procedure mainly includes two steps, i.e., i) thaw settlement test at an overburden pressure of lower than 1.0 kPa, and ii) step loads exerted on specimen after the deformation stabilized at the last stage. Thus, the consolidation of thawing soils can be empirically determined by Eq. (3).

$$S = A_0 h + \alpha P h \tag{3}$$

where, S is the total settlement of thawing soils (m); the first term in the right-hand side denotes the thaw settlement of soils at zero or small overburden pressure that was in general taken to be 1.0 kPa, with A_0 as the coefficient of thaw settlement and h the post-thawed depth while the second term is the compression of post-thawed domain, with overburden pressure, P and coefficient of compression α, which can be simply obtained from the compression curve, as can be noticed from Fig. 5.

The deformation corresponding to the break point A in Fig. 3, as can be easily determined from the compression curve, was taken to calculate the thaw-settlement coefficient of frozen saline soft clay and the remaining part considered as the consolidation under gravity and a small overburden pressure of 1.0 kPa. Fig. 6 gives the coefficient of thaw settlement for frozen saline soft clay at the considered test conditions. Clearly it can be seen that for specimens at the six salt contents, the coefficient of thaw settlement non-linearly increases with water content manifesting as lower value at relatively lower water contents, as shown in Fig. 6(a). Besides, an approximately linear increase was noted with salt content in logarithmic coordinate, as indicated from Fig. 6(b). At higher water contents, the gradient of thaw-settlement coefficient to salt content tends to grow while a lower value noticed at lower water contents. This may be related to the fact that the phase transition from crystalline salt into dissolved state also accounts for a part to the total deformation that cannot be neglected when investigating the thaw consolidation behaviors of frozen saline soils.

Experiments prove that the thaw-settlement coefficients for various types of soils such as cohesive soils, coarse-grained soils and muddy clay tend to increase as the amount of soil water grows. This primarily results from the shrinkage of soil pores that have been previously occupied by large ice crystal particles during thawing (Xu *et al.* 2001). However, as the water content is lower than or equal to a critical value, the soil may not exhibit obvious volumetric deformation during thawing, indicating that soil structure has not been considerably influenced during thawing. This critical value is regarded as the critical water content for thaw settlement, w_c, and can be obtained by following the method determining the coefficient of thaw settlement through a breakpoint at which two tangent lines intersect, as illustrated in Fig. 7. At higher salt contents, the critical water content in general decreases and little changes in the salt content will even cause a larger leap of the gradient of the critical water content to the salt content. While the gradient stabilized at higher salt contents. Moreover, the critical coefficient of thaw settlement, A_{ini}, corresponding to the critical water content w_c, also shows a nonlinear increase and the magnitude shows little change at larger salt contents. A power function was utilized here to describe the dependence of both critical water content of thaw settlement and corresponding critical thaw-settlement coefficient on salt contents. Better fitting results can be reached, with coefficient of correlation of larger than 0.80. The specific form is given in Eq. (4).

$$S = A_0 h + \alpha P h \tag{4}$$

where, y_i (i=1,2) represent the two characteristic indexes, i.e., critical water content of thaw settlement and critical coefficient of thaw settlement; α_1 and β_1 are fitted parameters determined by tests. For the tested specimens, α_1=27.527 , β_1=-0.229, α_2=0.566 , β_2=0.268.

Considering the practical significance of the critical water content of thaw settlement, both the coefficient of thaw settlement and water content obtained from test data

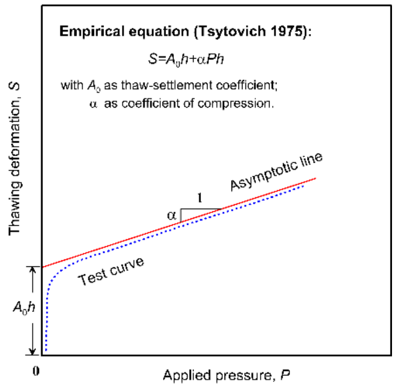

Fig. 5 Definition of thaw-settlement coefficient

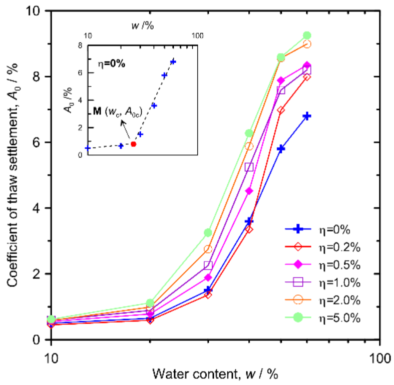

(a) Water content dependence

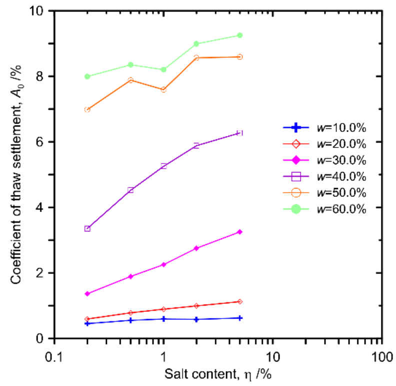

(b) Salt content dependence

Fig. 6 Thaw settlement coefficient of frozen saline soft clay

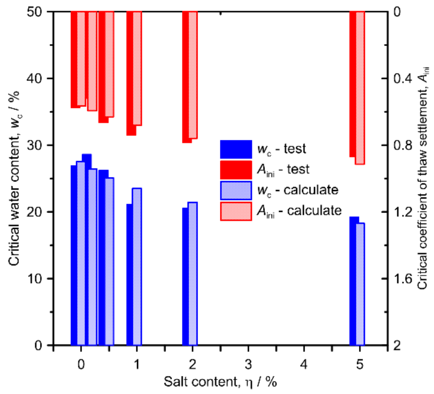

Fig. 7 The critical water content for thaw settlement of saline soft clay

was processed by using two new terms as an alternative such as A_0-A_{ini} and w-w_c, and the relationship between the two terms were plotted in Fig. 8. Here, the parameter A_{ini} denotes the critical coefficient of thaw settlement of frozen saline soft clay at a water content equal to the critical value, w_c. Clearly as the figure presents, the first term exhibits a good linear dependence on the second, and can be fitted by a proportional function. For specimens at six kinds of salt contents, the slope of each curve fitted from test results varies within a narrow range from 0.204 to 0.258 and the mean value of 0.231 can be used in the function. The fitting curves together with test data were both plotted in a graph and it is easily noted that the data points were closelydistributed along the y=x line, with the coefficient of correlation larger than 0.90, indicating a good fitting result for the salt contents considered here.

Thus, the following equation can be used.

$$A_0=\begin{cases} A_{ini} & ,w<w_c \\ \alpha\left(w-w_c\right)+A_{ini} & ,w\geq w_c \end{cases} \tag{5}$$

Substitute Eq. (4) into Eq. (5), we get Eq. (6) below.

$$A_0=\begin{cases} \alpha_1\left(S+1\right)^{\beta_1} & ,w<w_c \\ \alpha_1\left(S+1\right)^{\beta_1}+\alpha\left[w-\alpha_2\left(S+1\right)^{\beta_2}\right] & ,w\geq w_c \end{cases} \tag{6}$$

Substitute the variable into the above equation, and the coefficient of thaw settlement at various test conditions can be calculated. The comparison of calculated and measure

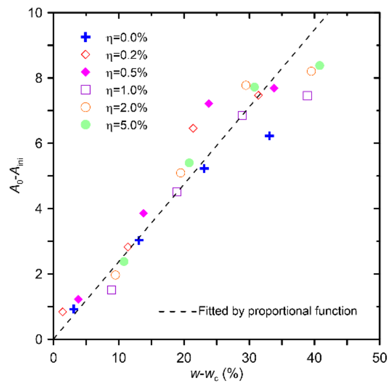

Fig. 8 Relation between thaw settlement coefficient and water content

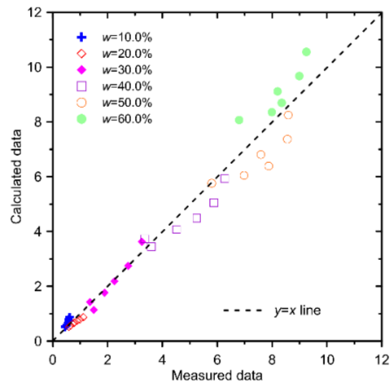

Fig. 9 Comparison of calculated and measured data

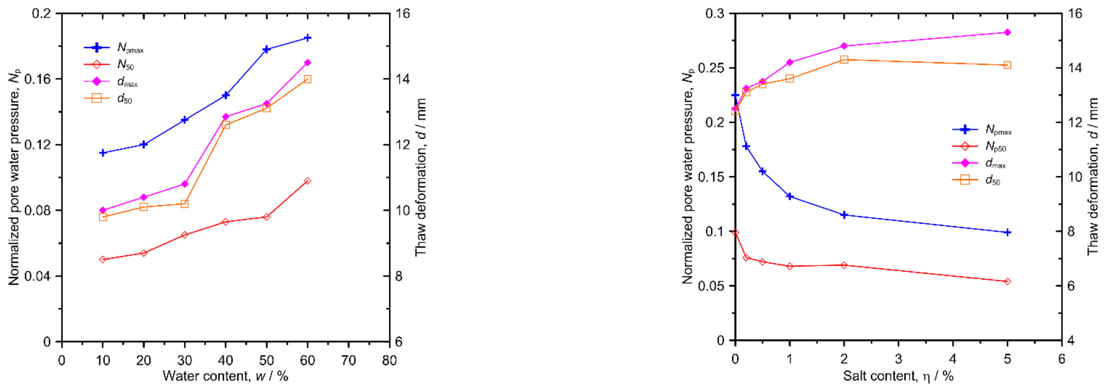

(a) Water content dependence (b) Salt content dependence

Fig. 10 Four characteristic parameters at various water-salt combinations

data illustrated in Fig. 9 indicates that most of the data points lies around the y=x line, and the calculated data agrees well with the test data. However, note that the proposed equation is applicable within the experimental conditions considered, but beyond this range, it still requires further verification, although we have considered the common water and salt contents and the freeze-thaw cycles.

3.3 Pore water pressure dissipation

Two characteristic indexes were defined based on test data for specimens at the second-level loading, i.e., normalized pore water pressure, N_{p50} and thawing deformation, d_{50}, with '50' representing 50% of the total test duration for the second stage. With two peak values considered here such as the maximum normalized pore water pressure, N_{pmax}, and maximum displacement, d_{max}, the consolidation of thawing saline soft clay at various water-salt combinations can be well reflected, as presented in Fig. 10. From Fig. 10(a), four characteristic parameters all tend to grow with the increase in the water content and more specifically, the parameters representing the deformation of thawing soils shows little difference in that consolidation of soils develops relatively slower at the two durations, with identical variations with water content. The peak value of the normalized pore water pressure, N_{pmax}, increases nonlinearly with the water content, manifesting as little change at lower water contents and rapidly increase as the soil water grows, based on which the conclusions can be drawn that the pore water pressure is more sensitive to the

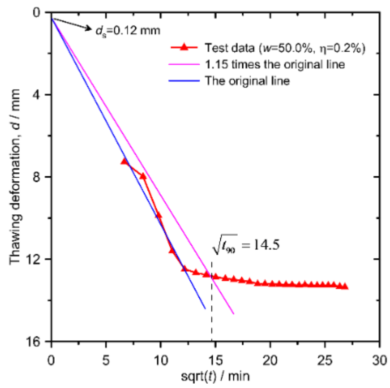

Fig. 11 Relationship between deformation and time square-root

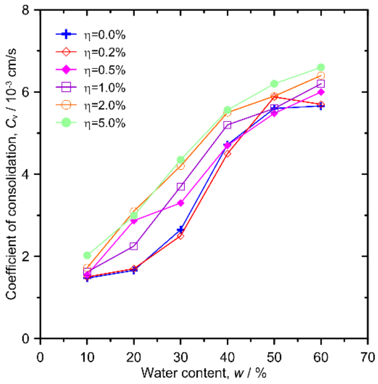

(a) Water content dependence

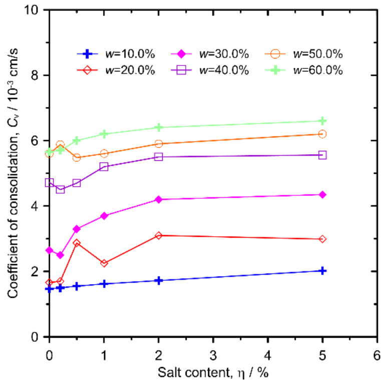

(b) Salt content dependence

Fig. 12 Coefficient of consolidation at various water-salt combinations

variation of water content. Besides, the normalized pore water pressure at time t_{50}, was slowly dissipated with consolidation of specimen and is not easily influenced by soil water. Moreover, the correlations of the four parameters with the salt content were given in Fig. 10(b). As the salt content increase, the deformation grows during thawing while the normalized pore water pressure due to the absorption of water by crystalline salt shows a slower dissipation at higher salt contents, and the magnitude of N_p also decreases with salt content.

The coefficient of consolidation at the second loading stage was obtained by a graphical method such as the square-root time method (Fig. 11). Firstly, the curves for consolidation of specimens was plotted in a graph with deformation and time square-root as the Y- and X-axes respectively. The initial linear segment of the measured data was extended until it intersects the Y-axis at point D (0, d_s), with d_s equal to 0.12 at w=50.0% and η=0.2%. A new curve with the X-axis of 1.15 times the original line was plotted in the graph. Both the new line and measured curve intersect at a new point, at which the degree of consolidation was regarded equal to 90% and the corresponding time is t_{90}. The coefficient of consolidation at this loading level can be calculated by Eq. (7).

$$C_v = 0.848\frac{\bar{h}^2}{t_{90}} \tag{7}$$

where, $\bar{h}$ is the distance of the maximum drainage path (m), equal to the mean value of the heights of specimen before and after a new load was applied. The characteristic time of t_{90} is equal to 210.25 min and the coefficient of consolidation, C_v, is equal to 5.88×10^{-3} cm/s after the two heights were substituted into Eq. (7). Based on the above method, the coefficients of consolidation at various water-salt combinations were obtained from test results and were given in Fig. 12. It indicates that at given salt content, the coefficient of consolidation for specimens at second-level loading tends to increase at higher water contents while for those at lower water contents, e.g., 30.0%, it has not been significantly influenced by the variation of water, as shown in Fig. 12(a). This may be related to the fact that the pore water pressure of specimen at lower water contents will be quickly balanced as the load is applied while for specimens at higher water contents the balance may take a longer time. From Fig. 12(b), the coefficient of consolidation has little correlation with the salt content of specimen, and only a small magnitude of increase can be noticed, proving that the consolidation of specimens at the second-level loading is primarily affected by the water content while the effect of salt inclusion can be neglected for sake of simplicity. A clue can also be found from the variation of the permeability of post-thawed specimens. After saturation in a vacuum condition, it changes in a narrow range from 1.45×10^{-8} to 5.35×10^{-8} m/s, i.e., in the same order of magnitude. It can be inferred from the above that the coefficient of thaw settlement is more sensitive to the salt content, if the possible collapsibility induced by the phase change of

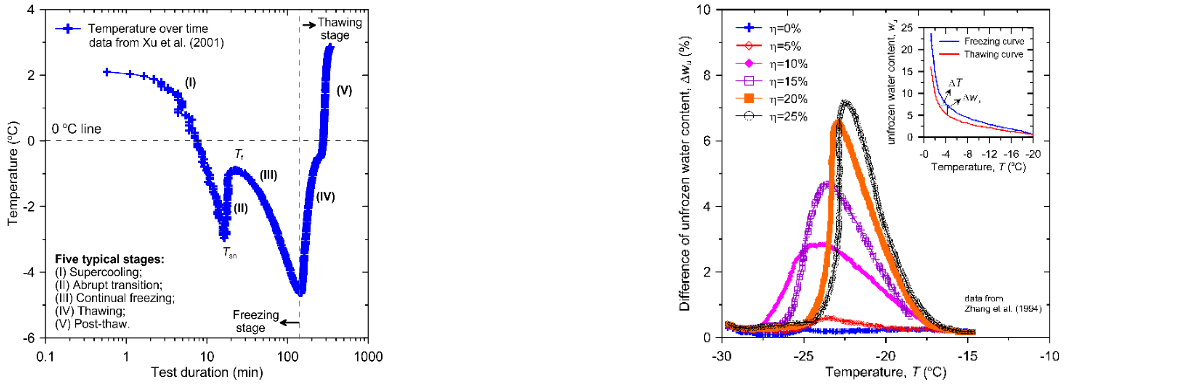

(a) Soil temperature changes over time

(b) Difference of unfrozen water content at various salt contents

Fig. 13 Variations of soil temperature with time and unfrozen water content during a freeze-thaw cycle

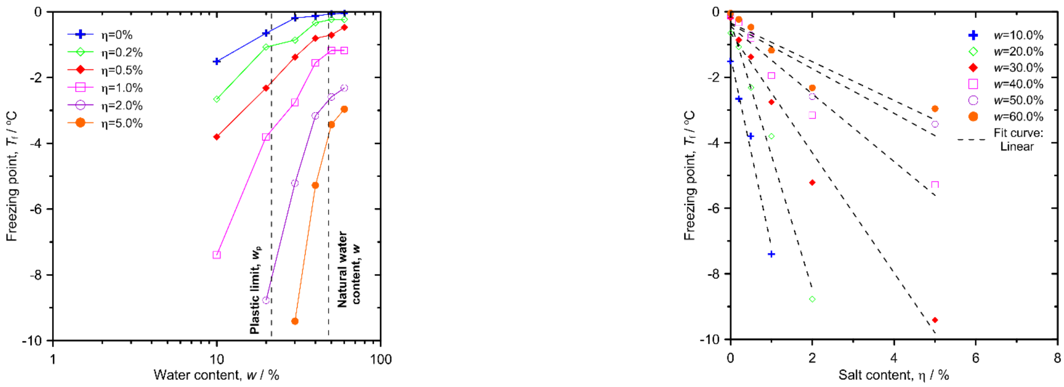

(a) Water content dependence

(b) Salt content dependence

Fig. 14 Effect of water-salt combination on soil freezing point

crystalline salt into the dissolved. Besides, after the second load is applied, part of the salt in soils has been discharged with the pore water, and thus the post-thawed specimen exhibits similar consolidation behavior to common soft clays, leading to a relatively stable consolidation coefficient.

3.4 Characteristic indexes affecting thawing of frozen saline soils

(1) Freezing point

From previous experiments on silty clay (Xu *et al.* 2001), the changes in soil temperature during a freeze-thaw cycle were plotted in Fig. 13(a). Clearly, three typical stages during freezing of soil specimen can be observed, i.e., (I) supercooling, (II) abrupt transition in soil temperature, and (III) continual freezing stages. In the supercooling section, the water in the soil is at a negative temperature, but no ice crystals appear. It is believed that the phase transition of liquid water in soil into solid ice primarily originates from the formation of the small molecular group, called the crystal center or germs. Then the molecular group grows into a slightly larger aggregate, called the nucleus that is finally combined or grown by small aggregates to produce ice crystals. The temperature at the center of the crystal is often lower than the freezing point, which leads to the occurrence of the supercooling section. An abrupt transition of soil temperature occurs at the second stage. The appearance of ice crystals causes the immediate release of latent heat, which causes the soil temperature to rise suddenly. In the third stage, that is, the continuous freezing stage, the water film becomes thinner, and the absorptive force of soil particles grows to bind water molecules. Note that a certain amount of salt is often present in the soil, and the concentration of the solution increases as the free water is absorbed by salt. Thus, the freezing point in this case continues to decline. It should be noted that the occurrence of the stable freezing phase is closely related to soil property and environmental conditions, and there is still a lack of a well-recognized mechanism to explain this problem (Guan *et al.* 2014), and thus, this point is not discussed here. Two stages are found from the thawing curve, i.e., thawing stage (IV) and post-thaw stage (V). As for the former, as the content of liquid water grows in frozen soil, the thawing temperature increases as well until the ice crystals are totally thawed, at which the second stage when thawing initiates, with soil temperature approaching to the ambient. A continual change in the curvature can also be observed from the temperature profile of the thawing process. However, it is undeniable that, in addition to determining the initial freezing temperature of the soil, it is difficult to accurately determine the thawing point of frozen soil as a positive temperature applied (Xu *et al.* 2001).

The top right corner of Fig. 13(b) shows the relationship between unfrozen water content and soil temperature during a freeze-thaw cycle. It indicates that the unfrozen water content measured during freezing is always higher than the data during thawing, i.e., a hysteresis phenomenon occurs (Zhang and Xu 1994). Provided that the thawing point can be selected from the temperature profile during thawing, more specifically, the breaking point of the thawing section, it is slightly higher than the freezing point. The difference was found to be correlated with various factors, e.g., the type and content of soluble salts (Xu *et al.* 2001). Because the difference of these two characteristic points is relatively small, the freezing point that can be simply determined from soil freezing curve is mostly used. Experiments also prove, as shown in Fig. 13(b), that the difference of unfrozen water content varies slightly, not higher than 1.0%, within the range of the salt content considered, i.e., 5.0%. Thus, the impact of the difference between the two can be neglected here.

Freezing of the soil generally occurs at a temperature lower than 0 ºC that has been frequently used in theoretical and numerical works to justify if soils are frozen or not, as found by many experiments (Qi *et al.* 2013, Yao *et al.* 2016). The second law of thermodynamics states that the entropy (a measure of the disorder) in a closed physical system never decreases. This implies that the temperature development during freezing and later thawing cannot be closed, and the hysteresis ring will occur after cyclic freeze and thaw. However, soil freezing point can also be utilized. Fig. 14 gives the freezing point of saline soft clay at considered water-salt combinations. At lower salt contents, the freezing point of saline soft clay shows a breakpoint at a water content close to the plastic limit, beyond which little change was observed. While a substantial increase occurred at water contents lower than this critical value, as can be found in Fig. 14(a). At higher salt contents, the increase in water content will significantly raise the freezing point, especially for cases when the water content is lower than the natural. This implies that for specimens at various salt contents, a critical water may exist beyond which the freezing point of soils will be limitedly influenced. This can be explained by the Gibbs-Thomson equation (Watanabe and Wake 2008), as shown below in Eq. (8).

$$T_m - T = \frac{T_m \sigma}{\rho_i L_f r} \tag{8}$$

where, T_m and T are freezing point of pure water at standard atmospheric pressure and capillary water (ºC); σ is the surface tension of ice-water (N/m); ρ_i is the density of ice (kg/m^3); L_f is the latent heat released during freezing of water (kJ/kg); r is the radius of capillaries (m).

It is found that the freezing point will be considerably lowered as the radius of capillaries is reduced. Besides, more unfrozen water exists for specimens at higher water contents, and this will lead to a relatively small magnitude of variation due to larger latent heat of ice-water phase change. Moreover, the gradient of soil freezing point to the water content, i.e., the slope of the curve, tends to grow at high salt contents. It can be deduced that the freezing point of saline soft clay is more sensitive to the changes in the water content at high salt contents, and is also correlated with the absorption of water by soil particles with cemented salt. As directly perceived from Fig. 14(b), the freezing point of saline soft clay approximately decreases linearly with the salt content. Bing and Ma (2011) has given an explanation that the reduction of freezing point is strongly dependent on the phase change of unfrozen water in soils that the cementation of soluble salt, and absorption, substitution and dispersion of ions occurred as the soluble salt is included, and besides, the soil water potential was also lowered due to the above processes. The salt inclusion added to the difficulty of accomplishing the phase change of unfrozen water.

(2) Heat conductivity

The coefficients of heat conductivity for soft clay at temperatures ranging from -20 to 20 ºC all decrease at higher salt contents, as shown in Fig. 15. The test data of specimen at a water content of 20.0% was taken as an example. Three typical stages can be easily noted from the curve, i) a slow decline stage with the heat conductivity of soft clay in frozen state changes insignificantly at lower temperatures; ii) an abrupt change stage at which thermal conductivity is quite sensitive to temperature and varies approximately linearly but within a narrow range; and iii) equilibrium stage at temperatures higher than the zero centigrade and thermal conductivity can be assumed as a constant in theories and numerical computation due to its lower sensitivity to temperature. Here we suggest using a constant in the two quasi-equilibrium stages when carrying out a geotechnical computation while a linear relation connecting with the two ends can be considered. Besides, the mean value of the two ends has already been employed in numerical works (Yao *et al.* 2012). The effect of latent heat release on the heat transfer of soil may be underestimated in this case. This may result from the three main modes of heat transfer, i.e., conduction, convection and radiation. Experiments prove that for extremely dry gravels, the radiation may account for a large proportion of the total and the free and force convection should also be concerned at higher void ratios in which case the heat loss may be larger (Xu *et al.* 2001). The heat conductivity measured has already included the contribution of the other two modes, not to mention the ice-water phase change.

Besides, the heat conductivity is not that influenced by salt content as more soluble salts are included. This also suggest that the increase in salt content will slow down the development of thawing boundary, corresponding to the temperature variation observed from test data. Due to the limited solubility of calcium chloride, the solution concentration increases positively with salt content at a given water content. According to the freezing point data at the above-mentioned salt contents, the difficulty in freezing the unfrozen water will raise. Freezing occurs at relatively low negative temperatures, resulting in a growth of the amount of unfrozen water in the soil. According to the standard thermal conductivity value of each component in the soil (Dong *et al.* 2015), the thermal conductivity of ice phase is about 4 times that of liquid water. Thus, the heat transfer efficiency will be lowered. Although the salt content is further increased, part of the calcium chloride will absorb unfrozen water with the precipitation of salt in the solution due to the decline of solubility at lower temperatures. As the solution content decreases, the heat conductivity will be further lowered. However, the figure

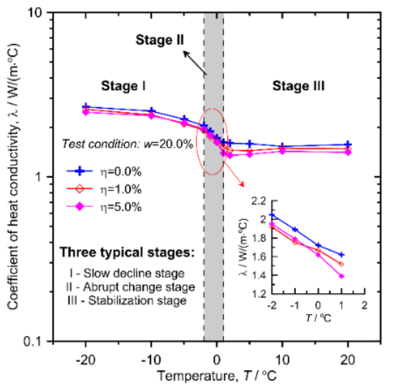

Fig. 15 Effect of salt content on heat conductivity of soft clay

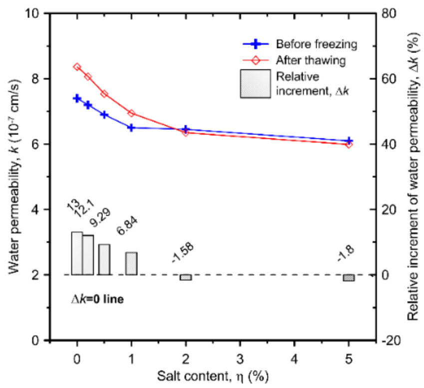

Fig. 16 Effect of salt content on water permeability of soft clay

also shows that as the salt content increases from 1.0% to 5.0%, the heat conductivity is not significantly reduced, which is related to the low water content of the soil. As for the subzero temperature section, i.e., stage I, a continual decrease in heat conductivity can be noted and two primary causes may account for this, i.e., 1) lowering solubility of calcium chloride as the temperature decreases, and ii) the freezing process of unfrozen solution at a temperature lower than its freezing point.

(3) Water permeability

Fig. 16 illustrates the relationship between water permeability and salt content for soft clay. It shows that the water permeabilities before freezing and after thawing tend to decrease slightly at higher salt contents, basically within the same order of magnitude, i.e., 10^{-7} cm/s. This may be related to the increase in the viscosity coefficient of the solution in soil pores. It is generally considered that the water permeability of clayey soils after freeze-thaw increases by several orders of magnitude (Qi *et al.* 2006). While for specimens tested in this study, it only slightly rises at salt contents lower than 2.0%, beyond which little change can be noticed. This also shows that the change of the permeation path of the specimen before and after freeze-thaw is not that obvious, implying that the deformation during freezing and that due to thawing can roughly compensate each other. The relative increment of water permeability was calculated, i.e., $\Delta k=(k_2-k_1)/k_1$, with k_1 and k_2 as the water permeability of specimens before freezing and after thawing at a given salt content. The gray histogram in Fig. 16 presents the variation of Δk with the salt content. Note that the symbols of '+' and '-' denote the growth and decline of the water permeability. Easily we can find that compared with the specimen before freezing, the magnitude of increase in the water permeability of specimen at a salt content of 2.0% ranges from 6.84% to 13.0%, while as the salt content exceeds this limit, only a slight decline lower than 2.0% occurs.

3.5 Changes in soil pore structure during thawing

(1) Pore volume changes

The mercury injection curves for saline soft clay can be roughly classified into three stages, as shown in Fig. 17(a), i.e., i) slow intrusion ($p \leq 50$ psia), ii) rapid intrusion ($50 < p \leq 20000$ psia), and iii) stabilization intrusion ($p > 20000$ psia). The mercury inflow pressure is relatively low in the first stage, and the amount of mercury injection slowly increases. The pressure of mercury in the second stage grows continuously, with an increasing cumulative mercury inflow. Besides, the increment of the amount of mercury injection and the logarithmic injection pressure gradually declines, reflecting the changes in mercury intrusion efficiency. During the third phase, the mercury intrusion pressure continues to increase, but the cumulative mercury intake gradually flattens and roughly enters a stable phase. Within the test conditions considered, the mercury ejection curves of the specimens generally exhibit consistent pattern, i.e., the amount of mercury ejection approximately linearly decreases with the logarithm of the mercury withdrawal pressure. The cumulative mercury intrusion corresponding to the ejection curve was higher than that of mercury injection. The two sections of the curves under the considered test conditions have not shown a closed pattern, indicating that the retention of mercury liquid occurs before and after mercury intrusion, and the residual amount may be related to the pore structure characteristics of the soil. By comparing the mercury injection and ejection curves of salt-free specimens before and after freeze-thaw, the volume of mercury injected tends to grow at higher logarithmic pressure of mercury intrusion. At the initial stage, i.e., the dividing point of between stages I and II (50 psia), the injection section of the curves tends to be overlapped. With the further increase in the injection pressure, the difference of the injection pressure for specimens before and after freeze-thaw grows. Also, the increment of the volume of mercury injected and the logarithmic injection pressure lowers. At an injection pressure of 20000 psia, i.e., the break point between stages II and III, the slope of the curve approaches to a constant with a relatively lower value. Moreover, the increment of the volume of mercury injected in stage III is higher than 0.5 mL/g compared with that before freezing. After the calcium chloride was mixed in the soil at salt contents of 0.5% and 5.0%, similar phenomena can also be observed in the mercury injection section, i.e., the mercury injection section of specimens after thawing is obviously higher than that before freezing. More obviously, the mercury intrusion curve of the specimen at high salt contents is slightly higher than that at low salt contents, indicating that the mercury intrusion pressure reduces as more salt is added, especially in the second and third stages

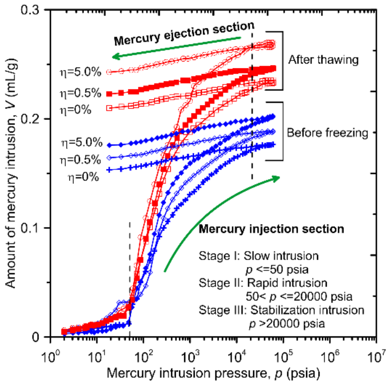

(a) V vs. p

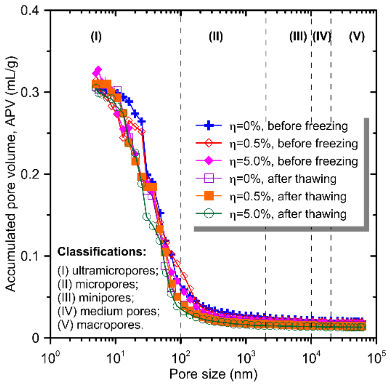

(b) APV vs. d

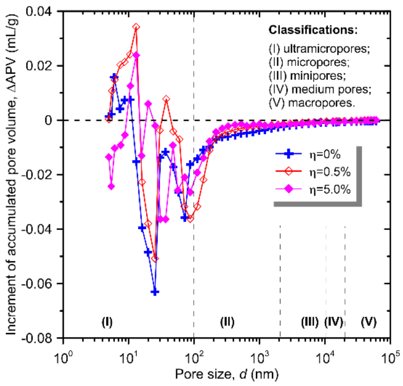

(c) ΔAPV vs. d

Fig. 17 Mercury intrusion test results for saline soft clay

of the curve. The mercury inflow in soils before and after freeze-thaw at different salt contents in the first stage were roughly overlapped, and the volume of mercury at lower mercury injection pressures did not change much.

The change in the volume of mercury injection actually reflects the pore volume characteristics of the soil. According to the Washburn equation (Webb 2001), the accumulated pore volume (APV) before and after freeze-thaw can be obtained, as illustrated in Fig. 17(b). Here, following the rules in classifying the pore size in soil (Shear *et al.* 1993; Wang *et al.* 2016c), five types of soil pores are considered based on the mercury intrusion tests, i.e., ultramicropores (d < 100 nm), micropores (100 < d < 2000 nm), minipores (2000 < d < 10000 nm), medium pores (10000 < d < 20000 nm), and macropores (d > 20000 nm). The pore size distribution curves of specimens at different salt contents manifest little difference before and after freeze-thaw, especially in the larger pore size range, e.g., d > 2000 nm. These curves generally overlap, indicating both salt content and freeze-thaw have little effect on the distribution of larger pores (i.e., minipores, medium pores and macropores). Within the range of ultramicropores and micropores, a pronounced change can be noted but the difference among the curves tends to decline. In order to more clearly show the effect of both salt content and freeze-thaw on pore size distribution, Fig. 17(c) presents the increment of accumulated pore volume (ΔAPV). Clearly it shows that the changes in the pore size mainly occurs in both the ultramicropores (d < 100 nm) and micropores (100 < d < 2000 nm), with the range of -0.08 - 0.04 mL/g while for the larger pores, little effect can be found. Besides, the ΔAPV changes little at the two considered salt contents. Compared with the salt-free specimens, after the calcium chloride at a content of 0.5% is added, the accumulated pore volume overall increases in the range of ultramicropores but a slight decrease in the micropores. As the salt content increases to 5.0%, the ΔAPV declines slightly, implying that a further increase in the salt content does not simply cause an increase in the APV.

Following the work by Wang *et al.* (2016c), i.e., the computational procedure based on the Housdroff method, the number of soil pores N_p with diameter larger than d can be described in Eq. (9).

$$N_p = \int_r^{\infty} p(d)\mathrm{d}d \propto r^{-D} \tag{9}$$

where, $p(d)$ is the density distribution function of pore size d; D is the fractal dimension of soil pores. Assuming soil pores are spherical, so the following function can be satisfied, i.e., Eq. (10).

$$V(d) = \int_0^r \frac{1}{6}\pi r^3 \mathrm{d}N_p \propto d^{3-D} \tag{10}$$

The total volume of soil pores, V, is introduced below in Eq. (11).

$$\frac{V(d)}{V} = \propto d^{3-D} \tag{11}$$

Thus, the fractal dimension, D, can be obtained from the accumulated pore volume distribution curves. Results show that at the three considered salt contents, the fractal dimension for specimens before freezing ranges from 2.665 to 2.673, with a mean value of 2.669. While for those after thawing, the range of fractal dimension is 2.640 - 2.652 with a mean value of 2.644. At higher salt contents, the fractal dimension of soil pore structure shows a slight decrease before and after freeze-thaw, and the data before freezing is slightly higher than that after thawing. However, it also shows from the data that the range of data variation is small, reflecting a limited effect of both the salt content and freeze-thaw on the pore structure.

Based on previous work by Qi *et al.* (2006), a substantial change in pore volume generally occurs in clayey soils, reflecting the disturbance of freeze-thaw to soil structure. However, for the saline soft clay tested in this study, the effect of salt inclusion on pore structure system is mainly concentrated in both ultramicropores and micropores, and soil pores in larger sizes are little affected by freeze-thaw. This may result from the fact that the medium of cemented particles increased as the salt was involved, and its effect on soil structure is not significant when there is no freezing or thawing. When the soluble salt is precipitated from the pore solution, the volume expansion of the soil due to the change of the salt from liquid to the solid state will disturb the connection and cementation between the particles, weakening the integrity of soil structure. After the frozen specimen is thawed, despite the volume reduction caused by the thawing of ice phase into liquid water, the crystalline salt is converted into the solution in the pores along with the phase change of water, which also causes the volume of the soil to decrease to a certain extent. The deformation is actually the result of the combination of thawing consolidation and collapsible deformation related to the soluble salt. As the external water is not available, that is, under the closed system, the difference in water content is not large, so the deformation caused by freeze and later thaw can roughly compensate each other. Thus, the pore structure of the soil specimen after freeze-thaw changes little compared with that before freezing.

4. Conclusions

This paper investigated the effect of salt content on thaw consolidation behavior of frozen saline soft clay, and both thawing deformation and pore water pressure dissipation were discussed. The heat and water migration during thawing of specimens were further analyzed by measuring three characteristic parameters, i.e., freezing point, heat conductivity and water permeability. The main conclusions are as follows.

- The critical water content for thaw settlement tends to grow at higher salt contents due to the absorption of unfrozen water by soil particle with cemented salt. The coefficient of thaw settlement increases at higher water contents, and the inclusion of soluble salt aggravates this kind of change. An empirical equation considering both water and salt contents was proposed by fitting test data.
- The normalized pore water pressure is taken as the basic index and it is found that the pore water pressure dissipation is influenced by both water and salt, manifesting that the normalized pore water pressure grows at higher water contents, especially when lower salt contents are considered. This is closely related to the dependence of both dynamic viscosity and freezing point on salt content.
- The development of temperature during thawing of specimens was affected by salt content, i.e., soil freezing point lowers at higher salt contents. The heat conductivity of specimen also decreases with salt content while the permeability of soils shows little correlation with the salt content and varies within the same order of magnitude, corresponding to the variation of the coefficient of consolidation.

Acknowledgments

This research was financially supported by the National Natural Science Foundation of China (Nos. 51778528, 41671061, 51878551, and 51574219), and the Importation and Development of High-Caliber Talents Project of Beijing Municipal Institutions granted to Dr. Jilin Qi (CIT&TCD20150101) These supports are greatly appreciated.

References

Bing, H. and Ma, W. (2011), “Laboratory investigation of the freezing point of saline soil”, *Cold Reg. Sci. Technol.*, **67**(1), 79-88. https://doi.org/ 10.1016/j.coldregions.2011.02.008.

Chen, X.S. (1996), “A “time-space” related design method of freezing wall”, *Coal Sci. Eng.*, **2**(2), 63-66.

Dong, Y., McCartney, J.S. and Ning, L. (2015), “Critical review of thermal conductivity model for unsaturated soils”, *Geotech. Geol. Eng.*, **33**(2), 207-221. https://doi.org/ 10.1007/s10706-015-9843-2.

Foriero, A. and Ladanyi, B. (1995), “FEM assessment of large-strain thaw consolidation”, *J. Geotech. Eng.*, **121**(2), 126-138. https://doi.org/ 10.1061/(ASCE)0733-9410(1995)121:2(126).

Grechishchev, S.E., Instanes, A., Sheshin, J.B., Pavlov, A.V. and Grechishcheva, O.V. (2001), “Laboratory investigation of the freezing point of oil-polluted soils”, *Cold Reg. Sci. Technol.*, **32**(2-3), 183-189. https://doi.org/ 10.1016/S0165-232X(01)00030-1.

Guan, H., Wang, D., Ma, W., Mu, Y.H., Wen, Z., Gu, T.X. and Wang, Y.T. (2014), “Study on the freezing characteristics of silty clay under high loading conditions”, *Cold Reg. Sci. Technol.*, **110**, 26-31. https://doi.org/10.1016/j.coldregions.2014.10.005.

Hildebrand, E.E. (1983), “Thaw settlement and ground temperature model for highway design in permafrost areas”, *Proceedings of the 4th International Conference on Permafrost*, Alaska, U.S.A., July. https://doi.org/ 10.1007/s12205-015-0419-8.

Karstunen, M., Wiltafsky, C., Krenn, H., Scharinger, F. and Schweiger, H.F. (2006), “Modelling the behaviour of an embankment on soft clay with different constitutive models”, *Int. J. Numer. Anal. Meth. Geomech.*, **30**(10), 953-982. https://doi.org/ 10.1002/nag.507.

Kozlowski, T. (2009), “Some factors affecting supercooling and the equilibrium freezing point in soil-water system”, *Cold Reg. Sci. Technol.*, **59**(1), 25-33. https://doi.org/10.1016/j.coldregions.2009.05.009.

Ma, W., Fang, L.L. and Qi J.L. (2011), “Methodology of study on freeze-thaw cycling induced changes in engineering properties of soils”, *Proceedings of the 9th International Symposium on Permafrost Engineering*, Mirny, Yakutia, Russia, September.

Marwan, A., Zhou, M., Abdelrehim, M.Z. and Meschke, G. (2016), “Optimization of artificial ground freezing in tunneling in the presence of seepage flow”, *Comput. Geotech.*, **75**, 112-125. https://doi.org/10.1016/j.compgeo.2016.01.004.

Morgenstern, N.R. and Nixon, J.F. (1971), “One-dimensional consolidation of thawing soils”, *Can. Geotech. J.*, **8**(4), 558-565. https://doi.org/ 10.1139/t71-057.

Nelson, P.P. (2016), “A framework for the future of urban underground engineering”, *Tunn. Undergr. Sp. Technol.*, **55**, 32-39. https://doi.org/ 10.1016/j.tust.2015.10.023.

Nelson, R.A., Luscher, U., Rooney J.W. and Stramler, A.A. (1983), “Thaw strain data and thaw settlement predictions for Alaskan soils”, *Proceedings of the 4th International Conference on Permafrost*, Alaska, U.S.A., July.

Nixon, J.F. and Morgenstern, N.R. (1973), “Practical extensions to a theory of consolidation for thawing soils”, *Proceedings of the*

2nd International Conference on Permafrost, Yakutsk, Russia, July.

Panday, S. and Corapcioglu, M.Y. (1995), "Solution and evaluation of permafrost thaw-subsidence model", *J. Eng. Mech.*, **121**(3), 460-469. https://doi.org/ 10.1061/(asce)0733-9399(1995)121:3(460).

Park, D. (2016), "Rate of softening and sensitivity for weakly cemented sensitive clays", *Geomech. Eng.*, **10**(6), 827-836. https://doi.org/ 10.12989/gae.2016.10.6.827.

Ponomarev, V.D., Sorokin, V.A. and Fedoseev, Y.G. (1988), "Compressibility of sandy permafrost during thawing", *Soil Mech. Found. Eng.*, **25**(3), 124-128. https://doi.org/ 10.1007/BF01709717.

Qi, J.L., Pieter, A.V. and Cheng, G.D. (2006), "A review of the influence of freeze-thaw cycles on soil geotechnical properties", *Permafrost Periglac.*, **17**, 245-252. https://doi.org/ 10.1002/ppp.559.

Qi, J.L., Yao, X.L. and Yu, F. (2013), "Consolidation of thawing permafrost considering phase change", *KSCE J. Civ. Eng.*, **17**(6), 1293-1301. https://doi.org/ 10.1007/s12205-013-0240-1.

Quang, N.D. and Giao, P.H. (2014), "Improvement of soft clay at a site in the Mekong Delta by vacuum preloading", *Geomech. Eng.*, **6**(5), 419-436. https://doi.org/ 10.12989/gae.2014.6.5.419.

Shear, D.L., Olsen, H.W. and Nelson, K.R. (1993), *Effects of Desiccation on the Hydraulic Conductivity versus Void Ratio Relationship for a Natural Clay*, Transportation Research Record, NRC National Academy Press, Washington, D.C., U.S.A.

Shoop, S. and Affleck, R. (2005), "Cap plasticity model for thawing soil. calibration of constitutive models", *J. Cold Reg. Eng.*, **3**, 139-150. https://doi.org/ 10.1061/40786(165)8.

Sykes, J.F., Lennox, W.C. and Charlwood, R.G. (1974), "Finite element permafrost thaw settlement model", *J. Geotech. Eng. Div.*, **100**(11), 1185-1201.

Tengborg, P. and Struk, R. (2016), "Development of the use of underground space in Sweden", *Tunn. Undergr. Sp. Technol.*, **55**, 339-341. https://doi.org/ 10.1016/j.tust.2016.01.002.

Tsytovich, N.A. (1975), *Mechanics of Frozen Soil*, McGraw-Hill, New York, U.S.A.

Vitel, M., Rouabhi, A., Tijani, M. and Guérin, F. (2016), "Thermo-hydraulic modeling of artificial ground freezing: Application to an underground mine in fractured sandstone", *Comput. Geotech.*, **75**, 80-92. https://doi.org/ 10.1016/j.compgeo.2016.01.024.

Von Wolffersdorff, P.A. (1996), "A hypoplastic relation for granular materials with a predefined limit state surface", *Mech. Cohes.-Frict. Mater. Struct.*, **1**(3), 251-271. https://doi.org/10.1002/(SICI)1099-1484(199607)1:3<251::AID-CFM13>3.0.CO;2-3.

Wang, D., Ma, W., Chang X.X. and Wang, A.G. (2005), "Study on the resistance to deformation of artificially frozen soil in deep alluvium", *Cold Reg. Sci. Technol.*, **42**(3), 194-200. https://doi.org/ 10.1016/j.coldregions.2005.01.006.

Wang, S.H. and Liu, F.Y. (2015), "A hypoplasticity-based method for estimating thaw consolidation of frozen sand", *Geotech. Geol. Eng.*, **33**(5), 1307-1320. https://doi.org/ 10.1007/s10706-015-9902-8.

Wang, S.H., Qi, J.L., Yu, F. and Liu, F.Y. (2016a), "A novel modeling of settlement of foundations in permafrost regions", *Geomech. Eng.*, **10**(2), 225-245. https://doi.org/ 10.12989/gae.2016.10.2.225.

Wang, W.L., Wang, L.M., Yu, F. and Wang, Q. (2016b), "One dimensional thaw consolidation behaviors with periodical thermal boundaries", *KSCE J. Civ. Eng.*, **20**(4), 1250-1258.

Wang, S.F., Yang, P., Liu, G.R. and Fan, W.H. (2016c), "Micro pore change and fractal characteristics of artificial freeze thaw soft clay", *Chin. J. Geotech. Eng.*, **38**(7), 1254-1261. https://doi.org/ 10.11779/CJGE201607012.

Wang, S.H., Wang, Q.Z., Qi, J.L. and Liu, F.Y. (2018), "Experimental study on freezing point of saline soft clay after freeze-thaw", *Geomech. Eng.*, **15**(4), 997-1004. https://doi.org/10.12989/gae.2018.15.4.997.

Watanabe, K. and Wake, T. (2008), "Hydraulic conductivity in frozen unsaturated soil", *Proceedings of the 9th International Conference on Permafrost*, Alaska, U.S.A., June-July.

Webb, P.A. (2001), *An Introduction to the Physical Characterization of Materials by Mercury Intrusion Porosimetry with Emphasis on Reduction and Presentation of Experimental Data*, Micromeritics Instrument Corporation, Norcross, Georgia, U.S.A.

Xu, J., Wang, Z., Ren, J. and Yuan, J. (2018), "Mechanism of shear strength deterioration of loess during freeze-thaw cycling", *Geomech. Eng.*, **14**(4), 307-314. https://doi.org/ 10.12989/gae.2018.14.4.307.

Xu, X.Z., Wang, J.C. and Zhang, L.X. (2001), *Frozen Soil Physics*, Science Press, Beijing, China.

Yao, X.L., Qi, J.L. and Wu, W. (2012), "Three dimensional analysis of large strain thaw consolidation in permafrost", *Acta Geotech.*, **7**(3), 193-202. https://doi.org/ 10.1007/s11440-012-0162-y.

Yao, X.L., Qi, J.L., Liu, M.X. and Yu, F. (2016), "Pore water pressure distribution and dissipation during thaw consolidation", *Transport Porous Med.*, **116**(2), 1-17. https://doi.org/ 10.1007/s11242-016-0782-z.

Yazdani, H. and Toufigh, M.M. (2012), "Nonlinear consolidation of soft clays subjected to cyclic loading–Part II: Verification and application", *Geomech. Eng.*, **4**(4), 243-249. https://doi.org/ 10.12989/gae.2012.4.4.243.

Yildiz, A. and Uysal, F. (2015), "Numerical modelling of Haarajoki test embankment on soft clays with and without PVDs", *Geomech. Eng.*, **8**(5), 707-726. https://doi.org/ 10.12989/gae.2015.8.5.707.

Zhang, L. and Xu, X. (1994), "The influence of freezing-thawing process on the unfrozen water content of frozen saline soil", *Proceedings of the 7th International Symposium on Ground Freezing*, Nancy, France, October.

CC